Cell Reports, Volume *43*

Supplemental information

The Janus kinase 1 is critical for pancreatic cancer initiation and progression

Hridaya Shrestha, Patrick D. Rädler, Rayane Dennaoui, Madison N. Wicker, Nirakar Rajbhandari, Yunguang Sun, Amy R. Peck, Kerry Vistisen, Aleata A. Triplett, Rafic Beydoun, Esta Sterneck, Dieter Saur, Hallgeir Rui, and Kay-Uwe Wagner

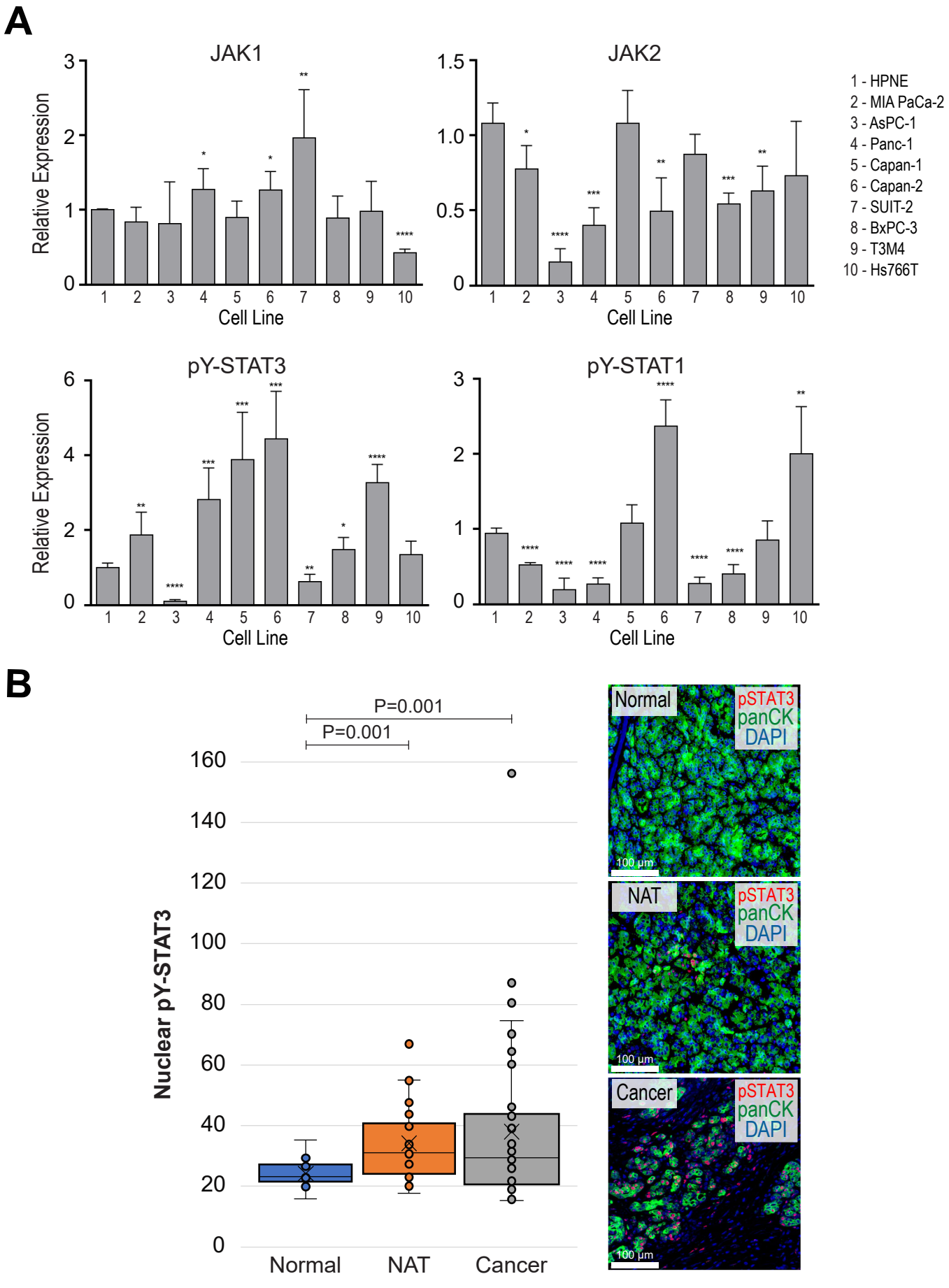
A
JAK1
JAK2
pY-STAT3
pY-STAT1
Relative Expression
Cell Line
1 - HPNE
2 - MIA PaCa-2
3 - AsPC-1
4 - Panc-1
5 - Capan-1
6 - Capan-2
7 - SUIT-2
8 - BxPC-3
9 - T3M4
10 - Hs766T
B
P=0.001
P=0.001
Nuclear pY-STAT3
Normal
NAT
Cancer
pSTAT3
panCK
DAPI
100 µm

Supplemental Figure S1. Elevated activation of STAT3 in untransformed pancreatic exocrine cells in the vicinity of primary tumors, Related to Figure 1

A. Relative normalized expression of JAK1 and JAK2 as well as tyrosine phosphorylated STAT3 and STAT1 in human pancreatic cancer cell lines (n=9) in comparison to the average value of two untransformed normal pancreatic cell lysates (HPNE1a/1b in Fig. 1A). The densitometry results for the individual JAK/STAT proteins from three immunoblots were normalized to the corresponding loading controls (beta-actin, ACTB). The bars represent the average expression from three technical repeats (±SD) in comparison to the protein levels in HPNE cells. Statistical significance was calculated with unpaired t-tests and *P*-values <0.05 (∗), <0.01 (∗∗), <0.001 (∗∗∗), and <0.0001 (∗∗∗∗) were considered statistically significant. **B.** Left: quantitative analysis of nuclear STAT3 expression on 29 pancreatic cancer cases, 20 normal pancreatic tissues adjacent to primary tumors (NAT), as well as 5 normal control pancreata. Right: immunofluorescent staining of tyrosine phosphorylated STAT3 (red) along with pan-cytokeratin (panCK, green) illustrating the presence of active STAT3 in pancreatic cancer cells (bottom) and a subset of normal cells adjacent to the primary tumors (middle). Active STAT3 was absent in most exocrine cells of normal pancreata (top). Slides were counterstained with DAPI; bars, 100 μm.

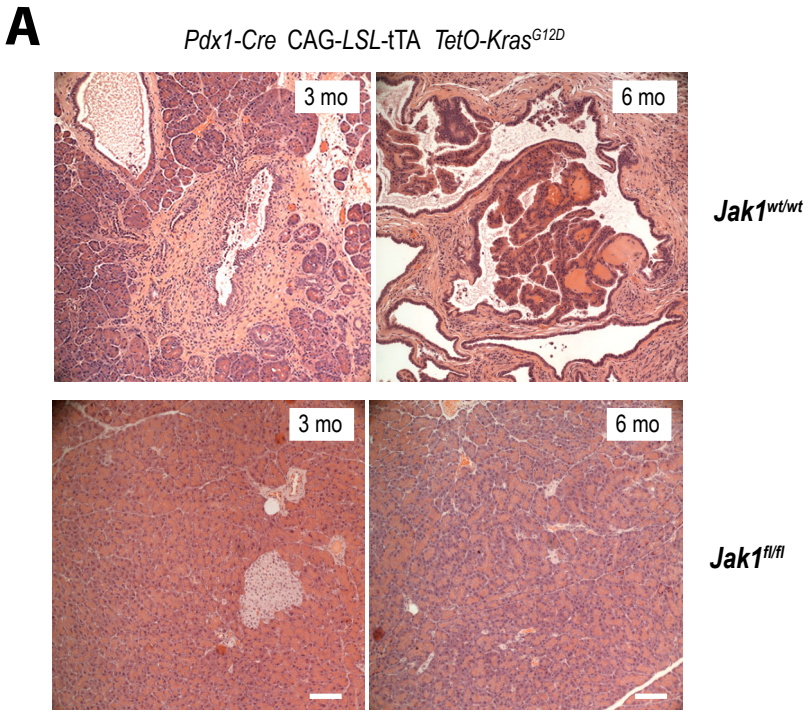
A
Pdx1-Cre CAG-LSL-tTA TetO-Kras^{G12D}
3 mo
6 mo
Jak1$^{wt/wt}$
3 mo
6 mo
Jak1$^{fl/fl}$

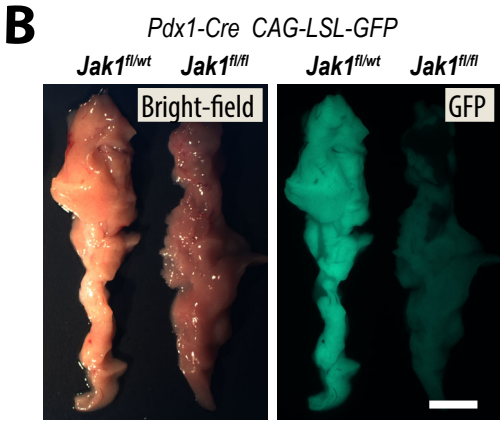
B
Pdx1-Cre CAG-LSL-GFP
Jak1$^{fl/wt}$
Jak1$^{fl/fl}$
Jak1$^{fl/wt}$
Jak1$^{fl/fl}$
Bright-field
GFP

Supplemental Figure S2. Lack of oncogenic $Kras^{G12D}$-indcued pancreatic tumor initiation in Pdx1-Cre-mediated JAK1 conditional knockout mice, Related to Figure 2

A. H&E-stained histologic sections of pancreata from 3- and 6-month-old transgenic mice that express mutant $KRAS^{G12D}$ in a tissue-specific and constitutive manner under the doxycycline-controlled transactivator (Pdx1-Cre CAG-LSL-tTA TetO-$Kras^{G12D}$) in a JAK1 wildtype (upper panel) or a JAK1 conditional knockout background (lower panel); bars, 100 µm. Note that the deletion of JAK1 and activation of the CAG promoter-driven transactivator (tTA) and oncogenic KRAS (TetO-$Kras^{G12D}$) in this model are codependent on the expression of the Pdx1-Cre. Consequently, the deletion of JAK1 occurs prior to neoplastic progression and a selective elimination of JAK1-deficient cells will likely eradicate cells that express the cancer-initiating oncogene. **B.** Representative stereoscopic brightfield and GFP fluorescent images of pancreata from adult mice that carry a GFP-based Cre/lox reporter (CAG-LSL-GFP) in addition to the Pdx1-Cre transgene in the presence of one or two *Jak1* conditional knockout alleles; bar, 0.5 cm. Note the significant reduction in GFP fluorescence in the Pdx1-Cre CAG-LSL-GFP transgenic mouse carrying two *Jak1* conditional knockout alleles ($Jak1^{fl/fl}$) in comparison to its litter mate control expressing JAK1 ($Jak1^{fl/wt}$) which is indicative of a selection against JAK1 knockout cells.

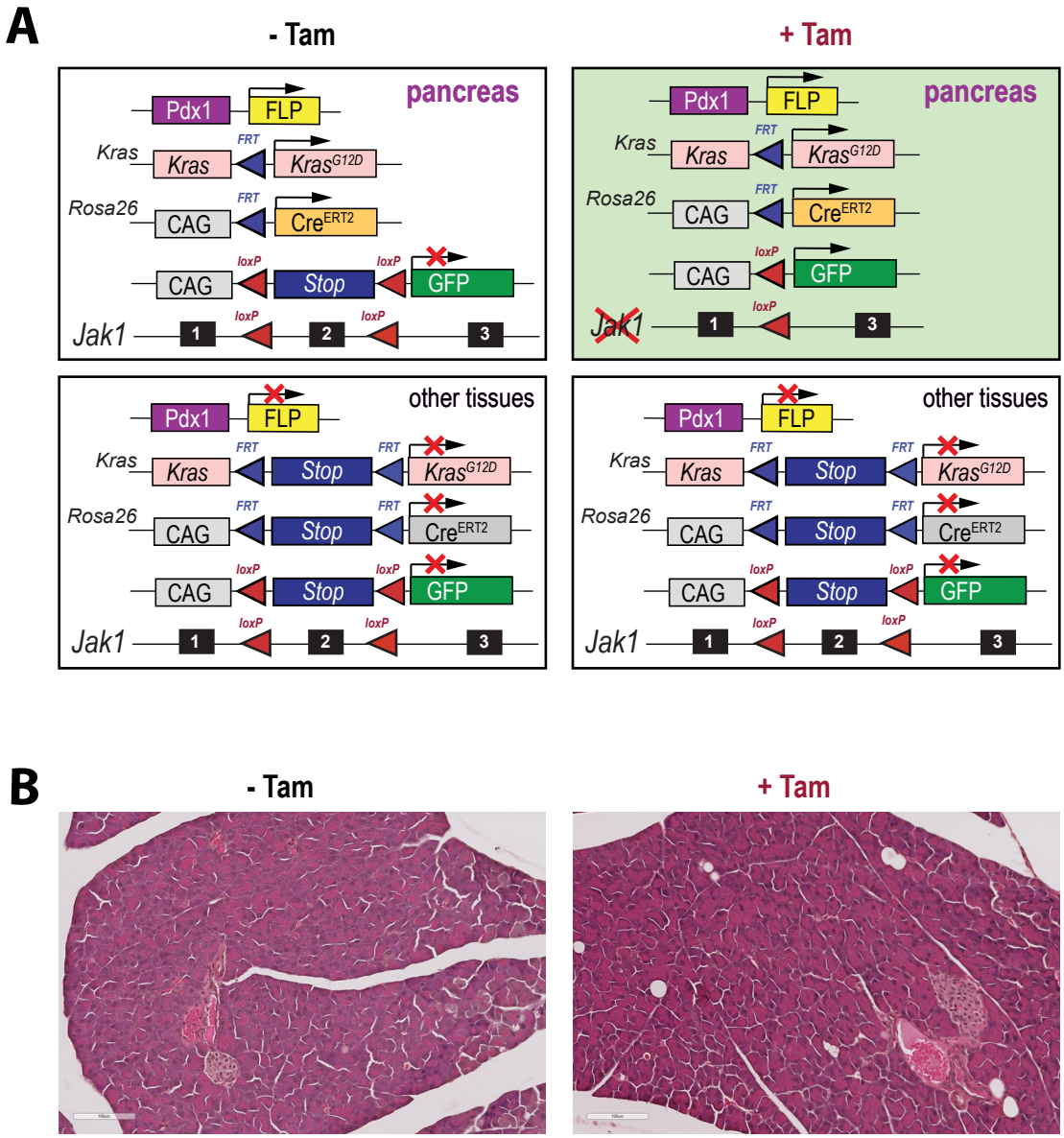
A
- Tam
+ Tam
pancreas
other tissues
Pdx1
FLP
Kras
FRT
Kras
Kras^G12D
Rosa26
CAG
Cre^ERT2
loxP
Stop
GFP
Jak1
1
2
3
B
- Tam
+ Tam

Supplemental Figure S3. A dual recombinase approach facilitates the activation of oncogenic KRAS and the conditional knockout of JAK1 in a temporally controlled manner, Related to Figure 2

A. Graphic illustration of the dual recombinase approach to coactivate oncogenic KRAS from its engineered endogenous locus (*FSF-Kras*^{G12D}) and tamoxifen-inducible Cre recombinase (Cre^{ERT2}) in pancreatic cells expressing the Pdx1-Flp transgene. The administration of tamoxifen (Tam) facilitates the conditional knockout of JAK1 in a ligand-inducible and temporally controlled manner. This feature allows the deletion of JAK1 in adolescent and adult mice independent of the initiation of KRAS^{G12D}-induced tumorigenesis. Expression of GFP from the Cre/lox reporter transgene (CAG-LSL-GFP) can be used to monitor the Flp-mediated expression and functionality of Cre^{ERT2} following the administration of Tam. **B.** H&E-stained histologic sections of pancreata from untreated (-Tam) or tamoxifen-treated (+Tam) mice that carry the Pdx1-Flp, *Rosa26*$^{CAG\text{-}FSF\text{-}CreERT2}$, and CAG-LSL-GFP transgenes in the presence of two *Jak1* conditional knockout alleles (*Jak1*$^{fl/fl}$), demonstrating the absence of obvious developmental defects following administration of Tam and deletion of JAK1.

A

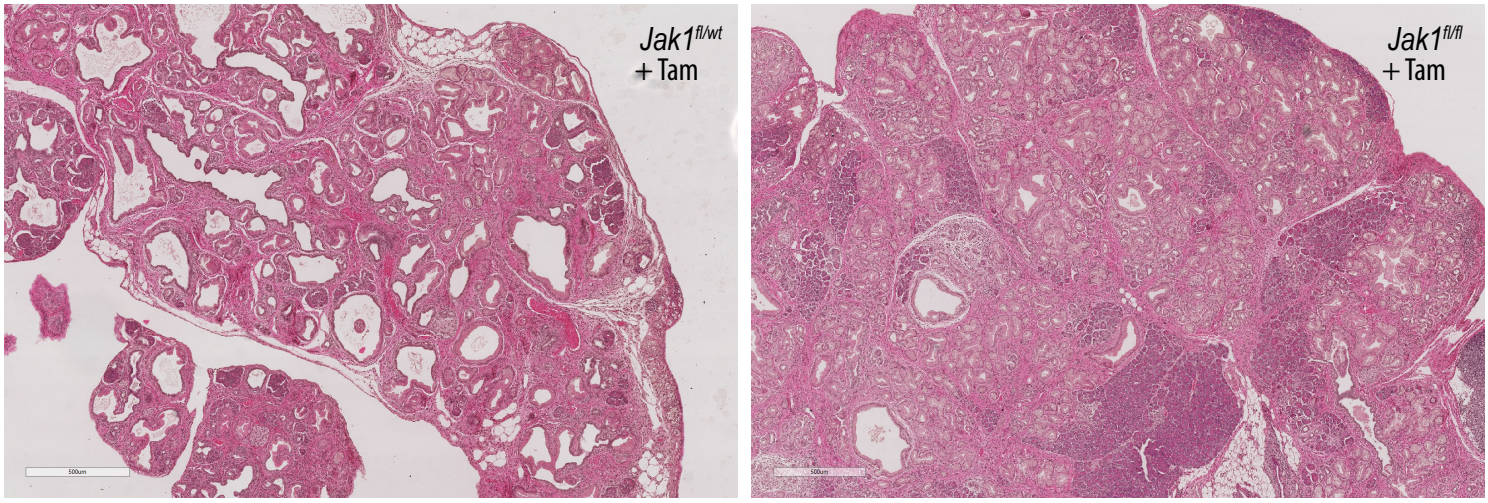
Jak1fl/wt
+ Tam
Jak1fl/fl
+ Tam

B

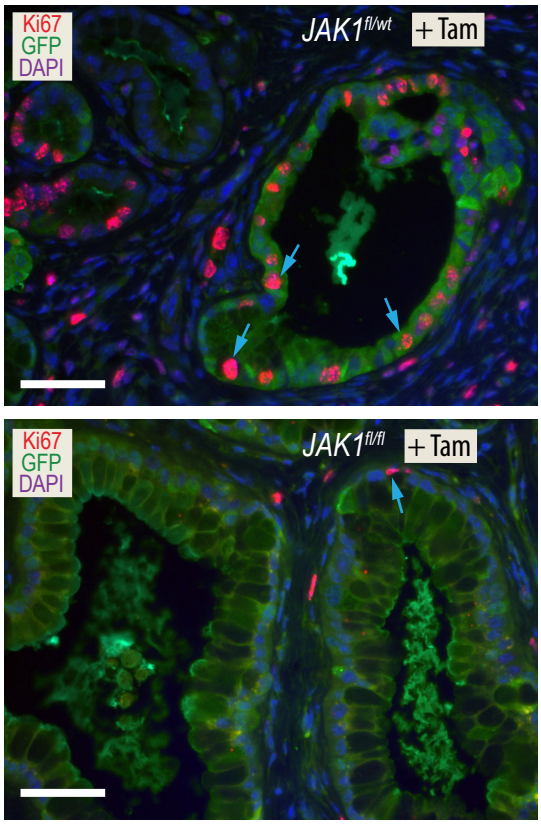
Ki67
GFP
DAPI
JAK1fl/wt
+ Tam
Ki67
GFP
DAPI
JAK1fl/fl
+ Tam

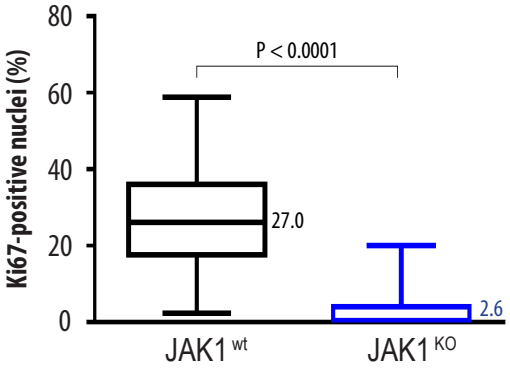
Ki67-positive nuclei (%)
80
60
40
20
0
P < 0.0001
27.0
2.6
JAK1 wt
JAK1 KO

Supplemental Figure S4. Low-grade PanINs deficient in JAK1 have a significantly reduced proliferation rate, Related to Figure 2

A. Low-magnification images of H&E-stained histologic sections of pancreata highlighting the widespread differences in the histopathology between a JAK1 conditional knockout (*Jak1*$^{fl/fl}$ + Tam) and a JAK1 expressing control animal (*Jak1*$^{fl/wt}$ + Tam) at 1 year of age, bars, 500 µm. **B**. Immunofluorescent staining of Ki-67 and GFP in pancreatic precursor lesions of the tissues shown in panel A. Blue arrows indicate the location of proliferating cells within GFP-positive (i.e., Cre^{ERT}-expressing) preneoplastic epithelial cells. DAPI was used as counterstain; bars, 50 µm. Note that the columnar cells of low-grade PanINs in JAK1 deficient mice are almost completely devoid of nuclear Ki-67 (*Jak1*$^{fl/fl}$ + Tam). The box plot of panel B illustrates the statistically significant difference in the relative number of Ki-67-positive nuclei between the JAK1 knockout and wildtype control. Ki-67-positive-nuclei in wildtype control are graphically represented by minimum = 2.381%, maximum = 58.82%, median = 26.19%, 25th percentile = 17.68%, 75th percentile = 35.94%, and the Ki-67-positive-nuclei in JAK1 knockout PanINs were graphically represented by minimum = 0.0%, maximum = 20%, median = 0.3571%, 25th percentile = 0.0%, 75th percentile = 4.082%. The statistical significance was calculated with a two-sided unpaired t-test, resulting in a *P*-value of <0.0001.

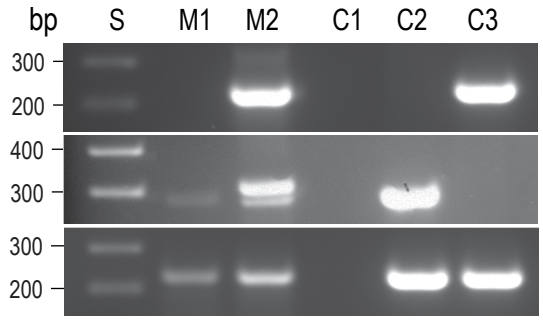

S DNA ladder

PDAC Metastases
M1 Adrenal gland tumor
M2 Adrenal gland tumor

Controls
C1 no DNA
C2 *Jak1* fl/fl
C3 Jak1 -/-

Supplemental Figure S5. PCR analysis to determine the presence of the unrecombined and Cre-mediated knockout alleles of *Jak1* in micro-dissected cancer cells from PDAC metastases to the adrenal glands of two JAK1 conditional knockout mice, Related to Figure 3

Note the absence or incomplete deletion of *Jak1* in both specimens. DNA control samples (C2, C3) were obtained from isogeneic pancreatic tumor cell lines before and after a retroviral-mediated deletion of both *Jak1* alleles.

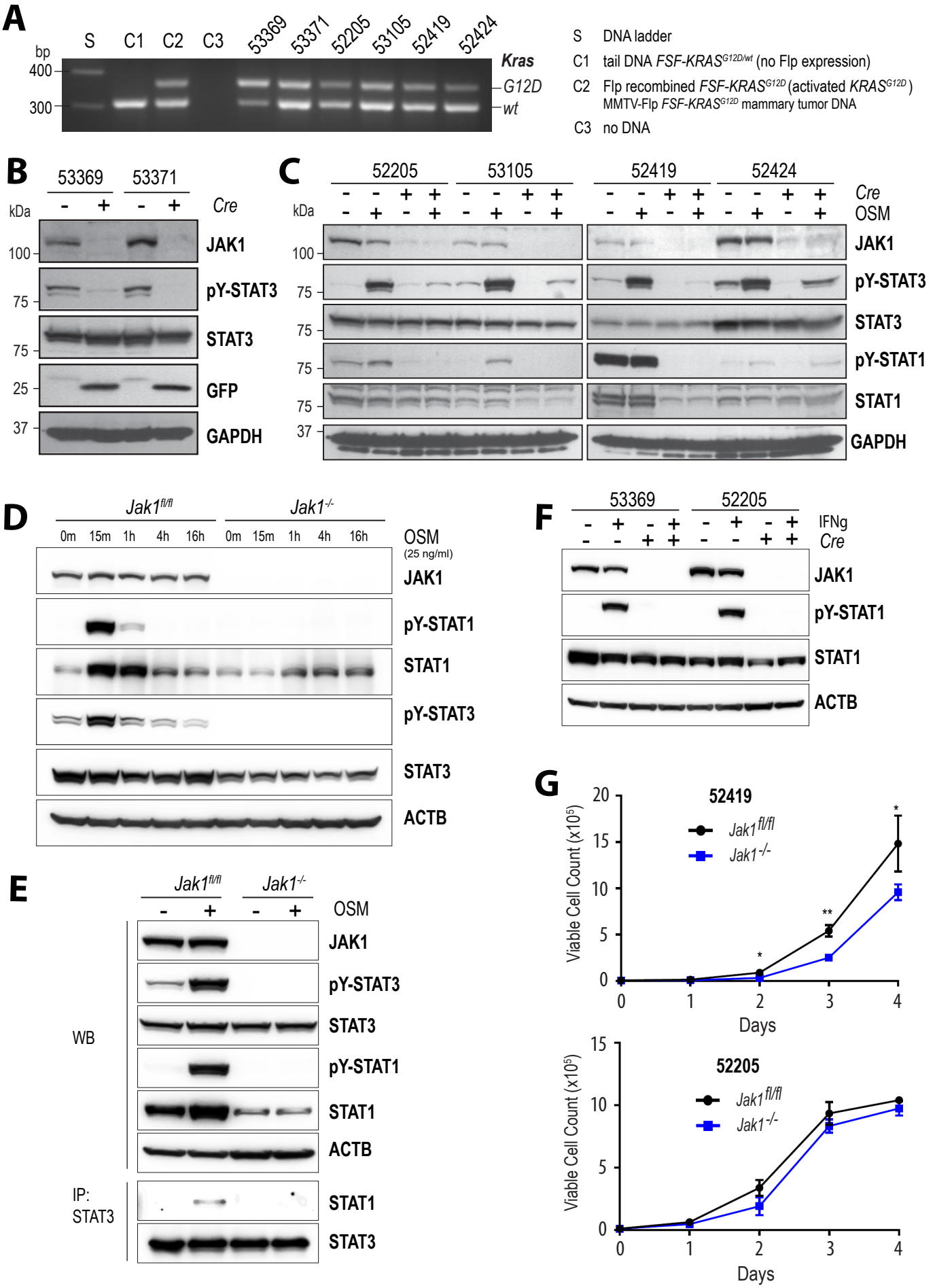
A
S C1 C2 C3 53369 53371 52205 53105 52419 52424
bp
400
300
Kras
G12D
wt
S DNA ladder
C1 tail DNA FSF-KRAS^G12D/wt (no Flp expression)
C2 Flp recombined FSF-KRAS^G12D (activated KRAS^G12D)
MMTV-Flp FSF-KRAS^G12D mammary tumor DNA
C3 no DNA
B
53369 53371
kDa
Cre
JAK1
pY-STAT3
STAT3
GFP
GAPDH
C
52205 53105 52419 52424
kDa
Cre
OSM
JAK1
pY-STAT3
STAT3
pY-STAT1
STAT1
GAPDH
D
Jak1fl/fl Jak1-/-
0m 15m 1h 4h 16h 0m 15m 1h 4h 16h
OSM
(25 ng/ml)
JAK1
pY-STAT1
STAT1
pY-STAT3
STAT3
ACTB
F
53369 52205
IFNg
Cre
JAK1
pY-STAT1
STAT1
ACTB
E
Jak1fl/fl Jak1-/-
OSM
WB
JAK1
pY-STAT3
STAT3
pY-STAT1
STAT1
ACTB
IP: STAT3
STAT1
STAT3
G
52419
Jak1fl/fl
Jak1-/-
Viable Cell Count (x10^5)
Days
52205
Jak1fl/fl
Jak1-/-
Viable Cell Count (x10^5)
Days

Supplemental Figure S6. Isogenic mouse pancreatic tumor cell lines with and without JAK1 reveal a pivotal role for JAK1 in the constitutive activation of STAT3 and STAT1, Related to Figure 4

A. PCR assay to validate the presence of the Flp-activated *Kras*^{G12D} allele in the parental pancreatic tumor cell lines (n=6). **B.-E.** Immunoblot analyses to assess the lack of JAK1 in cells expressing Cre recombinase as well as resulting changes in STAT3 and STAT1 activation at steady-state (B) or in response to Oncostatin M (OSM) stimulation (C-E). Note the low abundance of STAT3/1 heterodimers at the time of highest STAT activation following 15 minutes of OSM treatment (D,E). **F**. JAK1 is essential for the interferon gamma (IFNg)-mediated activation of STAT1. GAPDH and ACTB were used as loading controls on all immunoblots. **G**. Viable cells count in monolayer cultures of two isogenic tumor cell lines with and without JAK1. The data points shown represent mean values of cell counts ±SD. Statistical significance was calculated for each time point with t-tests; P-values <0.05 (*) and <0.01 (**).

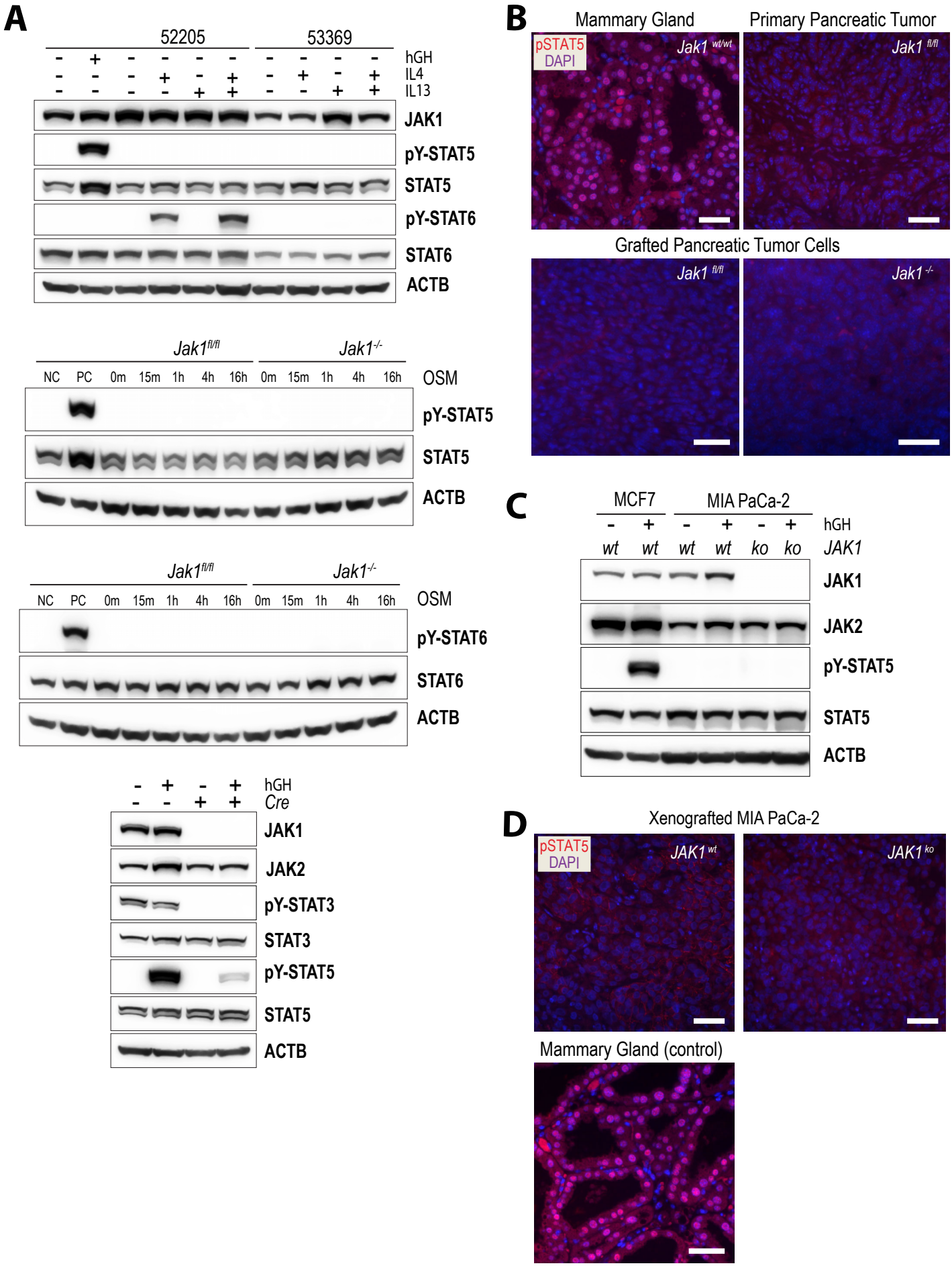
A
52205
53369
hGH
IL4
IL13
JAK1
pY-STAT5
STAT5
pY-STAT6
STAT6
ACTB
Jak1fl/fl
Jak1-/-
NC PC 0m 15m 1h 4h 16h 0m 15m 1h 4h 16h
OSM
pY-STAT5
STAT5
ACTB
Jak1fl/fl
Jak1-/-
NC PC 0m 15m 1h 4h 16h 0m 15m 1h 4h 16h
OSM
pY-STAT6
STAT6
ACTB
hGH
Cre
JAK1
JAK2
pY-STAT3
STAT3
pY-STAT5
STAT5
ACTB
B
Mammary Gland
Primary Pancreatic Tumor
pSTAT5
DAPI
Jak1 wt/wt
Jak1 fl/fl
Grafted Pancreatic Tumor Cells
Jak1 fl/fl
Jak1 -/-
C
MCF7
MIA PaCa-2
hGH
wt wt wt wt ko ko
JAK1
JAK1
JAK2
pY-STAT5
STAT5
ACTB
D
Xenografted MIA PaCa-2
pSTAT5
DAPI
JAK1 wt
JAK1 ko
Mammary Gland (control)

Supplemental Figure S7. Cytokine response studies to assess the activation of STAT5 and STAT6 in isogenic pancreatic cancer cell lines with and without JAK1, Related to Figure 4

A., **C.** Immunoblot analyses to determine the activation of STAT5 and STAT6 in response to stimulation with IL-4, IL-13, OSM, and hGH. Negative and positive controls (NC, PC) in panel A were mouse pancreatic cancer cells before and after stimulation with hGH (pSTAT5) and IL-4 (pSTAT6). MCF7 cells served as a control for the hGH-mediated activation of human STAT5 in panel C. Beta-actin (ACTB) was used as a loading control on all immunoblots. **B**., **D**. Immunofluorescent staining of active STAT5 in engrafted mouse (B) and human (D) pancreatic cancer cells with a targeted deletion of JAK1 and their parental JAK1-expressing controls. Mammary gland tissues from lactating mice served as controls. Note that JAK1 deficiency and consequential loss of STAT1, 3, and 6 activation does not lead to a compensatory activation of STAT5 *in vitro* and *in vivo*. Unlike human MCF7 breast cancer cells, MIA PaCa-2 pancreatic cancer cells are unresponsive to growth hormone to activate STAT5.

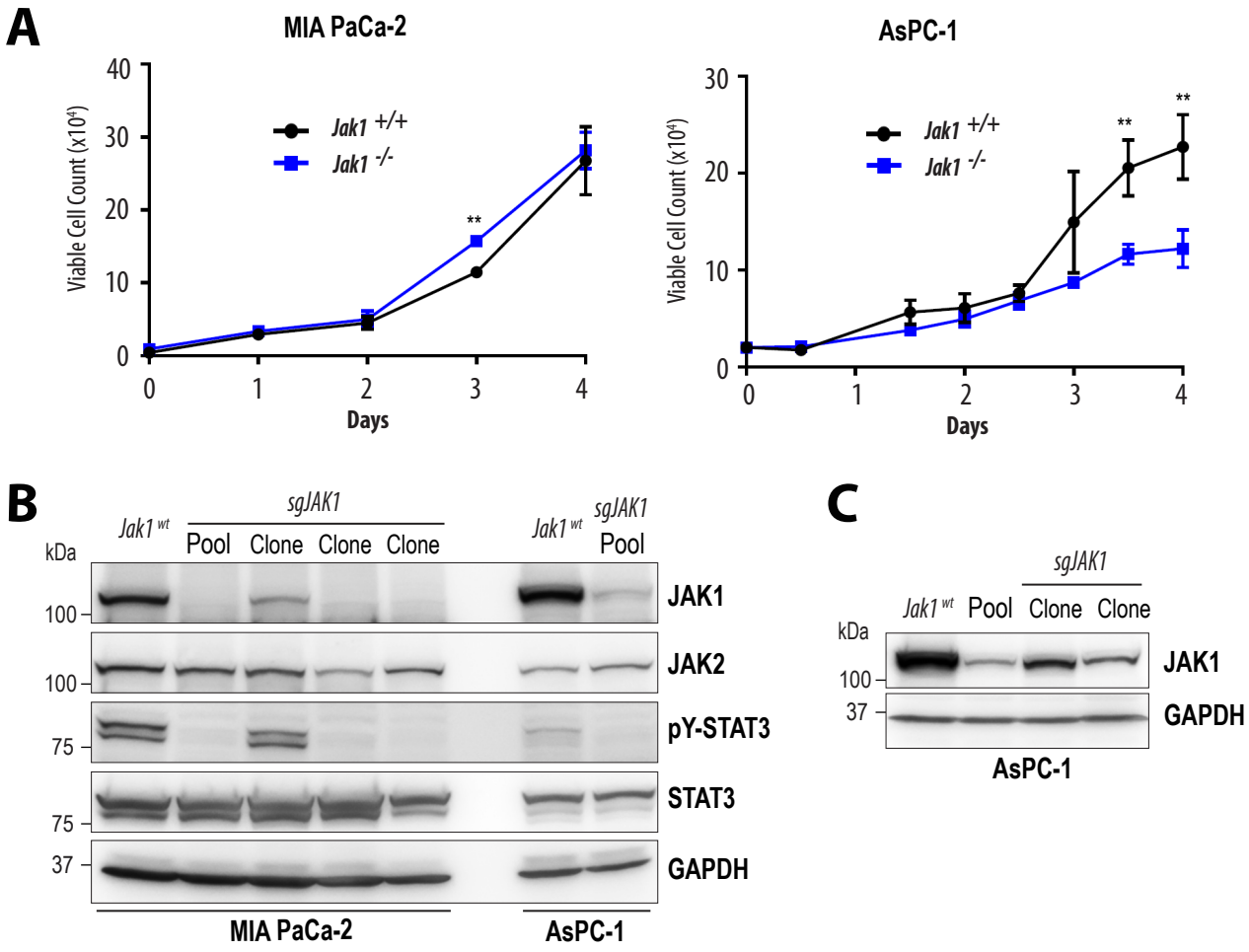
A
MIA PaCa-2
Viable Cell Count (x10⁴)
Jak1 +/+
Jak1 -/-
**
Days
AsPC-1
B
Jak1 wt
sgJAK1
Pool
Clone
Clone
Clone
Jak1 wt
sgJAK1
Pool
kDa
100
JAK1
100
JAK2
75
pY-STAT3
75
STAT3
37
GAPDH
MIA PaCa-2
AsPC-1
C
sgJAK1
Jak1 wt
Pool
Clone
Clone
kDa
100
JAK1
37
GAPDH
AsPC-1

Supplemental Figure S8. The generation of human pancreatic cancer cell lines with a CRISPR/Cas9-mediated knockout of the *JAK1* gene, Related to Figures 4

A. Viable cell counts of parental MIA PaCa-2 and AsPC-1 cells and their unselected (i.e., pooled) JAK1-deficient derivatives following a CRISPR/Cas9-mediated knockout of *JAK1*. The data points shown represent mean values of cell counts ±SD. Statistical significance was calculated for each time point with t-tests; P-values <0.05 (*) and <0.01 (**). **B.** and **C.** Immunoblot analyses to assess the efficiency of the JAK1 knockout in MIA PaCa-2 and AsPC-1 cells (pooled cells) and STAT3 activation in clonal derivatives. GAPDH was used as a loading control.

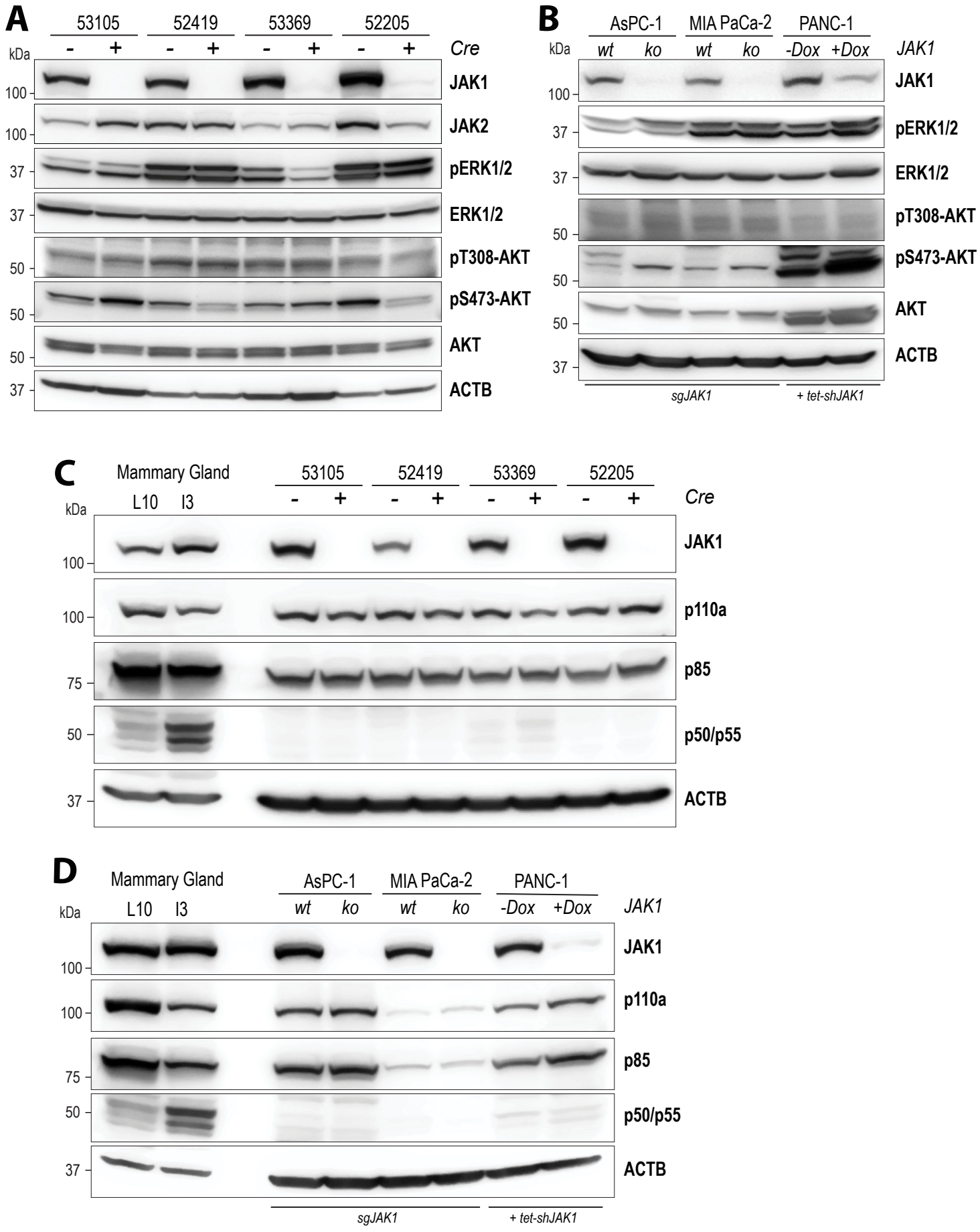
A
53105
52419
53369
52205
kDa
- + - + - + - +
Cre
100
JAK1
100
JAK2
37
pERK1/2
37
ERK1/2
50
pT308-AKT
50
pS473-AKT
50
AKT
37
ACTB
B
AsPC-1
MIA PaCa-2
PANC-1
kDa
wt ko wt ko -Dox +Dox
JAK1
100
JAK1
37
pERK1/2
37
ERK1/2
50
pT308-AKT
50
pS473-AKT
50
AKT
37
ACTB
sgJAK1
+ tet-shJAK1
C
Mammary Gland
L10 I3
53105
52419
53369
52205
kDa
- + - + - + - +
Cre
100
JAK1
100
p110a
75
p85
50
p50/p55
37
ACTB
D
Mammary Gland
L10 I3
AsPC-1
MIA PaCa-2
PANC-1
kDa
wt ko wt ko -Dox +Dox
JAK1
100
JAK1
100
p110a
75
p85
50
p50/p55
37
ACTB
sgJAK1
+ tet-shJAK1

Supplemental Figure S9. The expression and activation of MAP kinase and PI3 kinase signaling are not significantly altered in mouse and human pancreatic cancer cells, Related to Figure 6

A. and **B.** Immunoblot analyses to assess the activation of ERK1/2 and AKT in four isogenic mouse PDAC cell lines before and after Cre-mediated deletion of *Jak1* (A) as well as three human pancreatic cancer cell lines (B) with a gene-edited excision of *JAK1* (AsPC-1, MIA PaCa-2) or shRNA-mediated knockdown of this Janus kinase in a doxycycline (Dox)-dependent manner (PANC-1). **C.** and **D.** Expression analysis of the catalytic and regulatory subunits of the PI3 kinase in mouse (C) and human (D) pancreatic cancer cells with and without JAK1. Actin (ACTB) served as a loading control. Mammary gland tissues from lactating (L10, lactation day 10) and involuting mice (I3, involution day 3) served as controls. Note the significant upregulation of p50/p55 during mammary gland involution but the complete absence of these PI3K subunits in all mouse (n=4 biological replicates) and human pancreatic cancer cell lines (n=3 biological replicates).

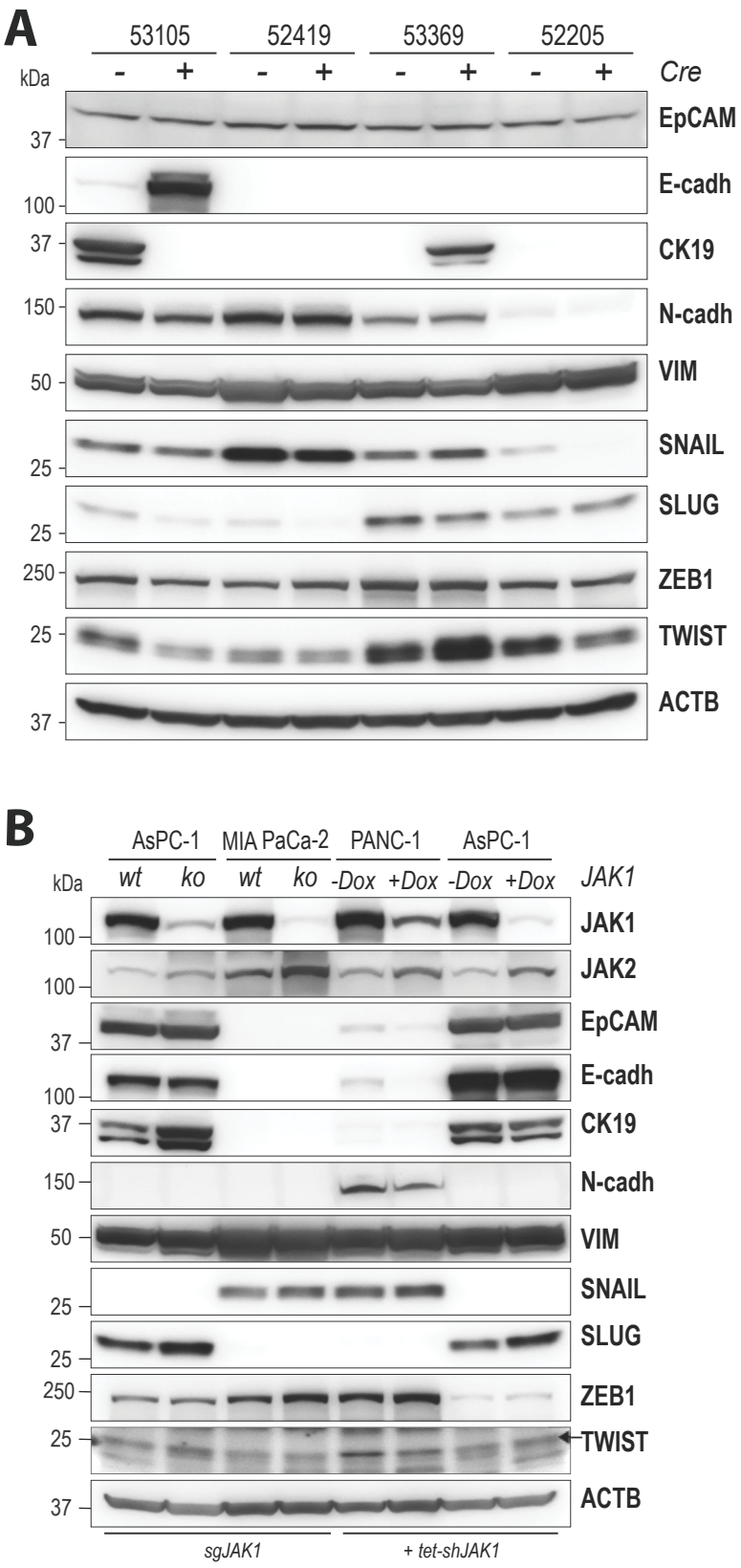
A
53105
52419
53369
52205
kDa
- + - + - + - +
Cre
EpCAM
E-cadh
CK19
N-cadh
VIM
SNAIL
SLUG
ZEB1
TWIST
ACTB
37
100
37
150
50
25
25
250
25
37
B
AsPC-1
MIA PaCa-2
PANC-1
AsPC-1
kDa
wt ko wt ko -Dox +Dox -Dox +Dox
JAK1
JAK1
JAK2
EpCAM
E-cadh
CK19
N-cadh
VIM
SNAIL
SLUG
ZEB1
TWIST
ACTB
100
100
37
100
37
150
50
25
25
250
25
37
sgJAK1
+ tet-shJAK1

Supplemental Figure S10. Lack of JAK1/STAT signaling does not affect common regulators of cellular plasticity, Related to Figure 6

Immunoblot analyses to assess the expression of epithelial and mesenchymal markers or transcription factors that are known regulators of cellular plasticity in four isogenic mouse PDAC cell lines before and after Cre-mediated deletion of *Jak1* (**A**) as well as three human pancreatic cancer cell lines (**B**) with a gene-edited excision of *JAK1* (AsPC-1, MIA PaCa-2) or shRNA-mediated knockdown of this Janus kinase in a doxycycline (Dox)-dependent manner (PANC-1, AsPC-1). Actin (ACTB) served as a loading control.

A

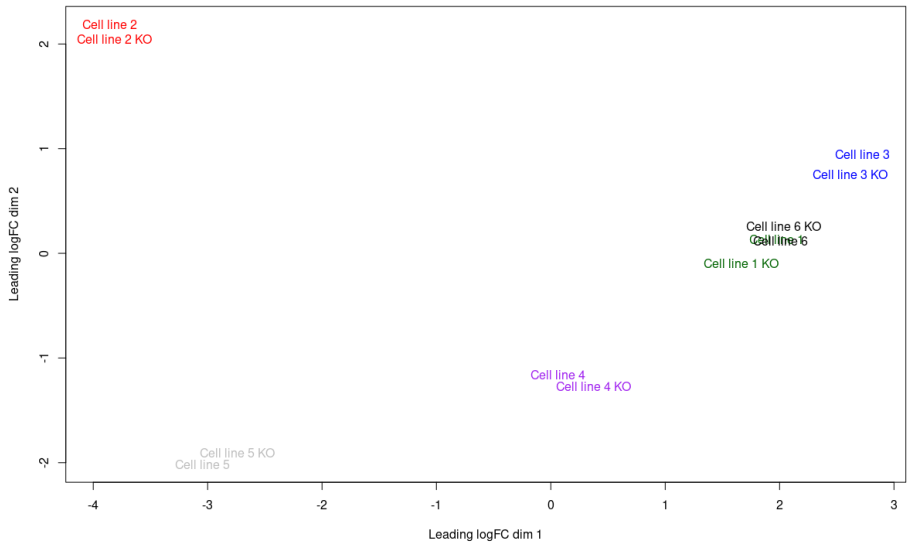
Cell line 2
Cell line 2 KO
Cell line 3
Cell line 3 KO
Cell line 6 KO
Cell line 6
Cell line 1 KO
Cell line 4
Cell line 4 KO
Cell line 5 KO
Cell line 5
Leading logFC dim 2
Leading logFC dim 1
2
1
0
-1
-2
-4
-3
-2
-1
0
1
2
3

B

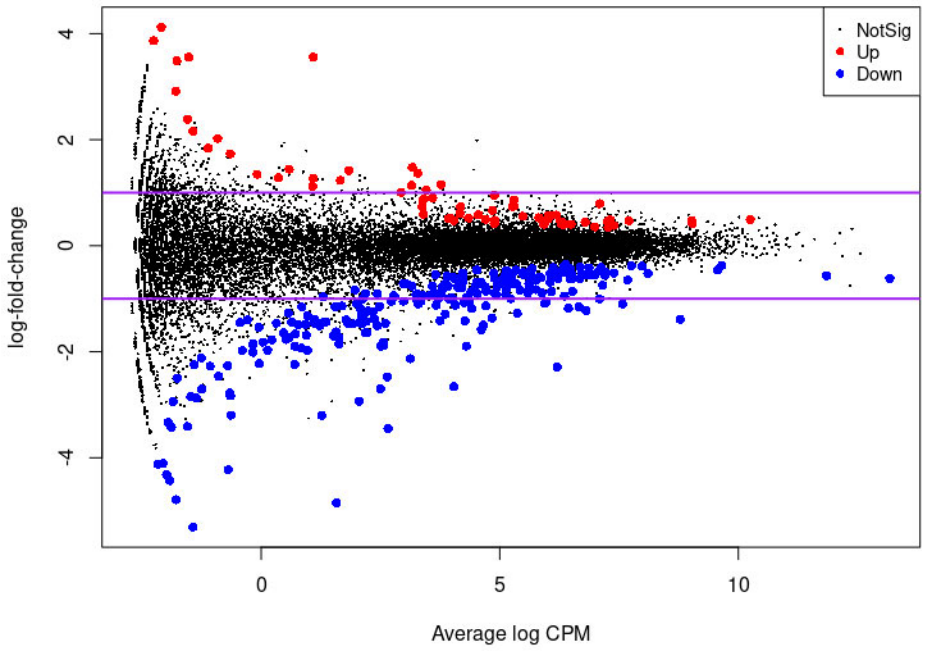
NotSig
Up
Down
log-fold-change
Average log CPM
4
2
0
-2
-4
0
5
10

Supplemental Figure S11. RNA sequencing analysis to assess the heterogeneity of expression profiles between mouse pancreatic cancer cell lines and to determine differences in gene expression caused by the knockout of JAK1, Related to Figure 6

A. Multi-dimensional scaling (MDS) plot of RNA-sequencing data of six isogenic pairs of mouse pancreatic cancer cell lines before and after Cre-mediated deletion of JAK1. Note the close location of isogenic lines on the plot, suggesting that gene expression differences between tumor cell lines from different mice are greater than the differences in each isogenic cell line pair caused by JAK1 deficiency. **B.** Plot illustrating the differential gene expression landscape resulting from the paired RNA-seq analysis of the parental cell lines and their JAK1 knockout derivatives.

A

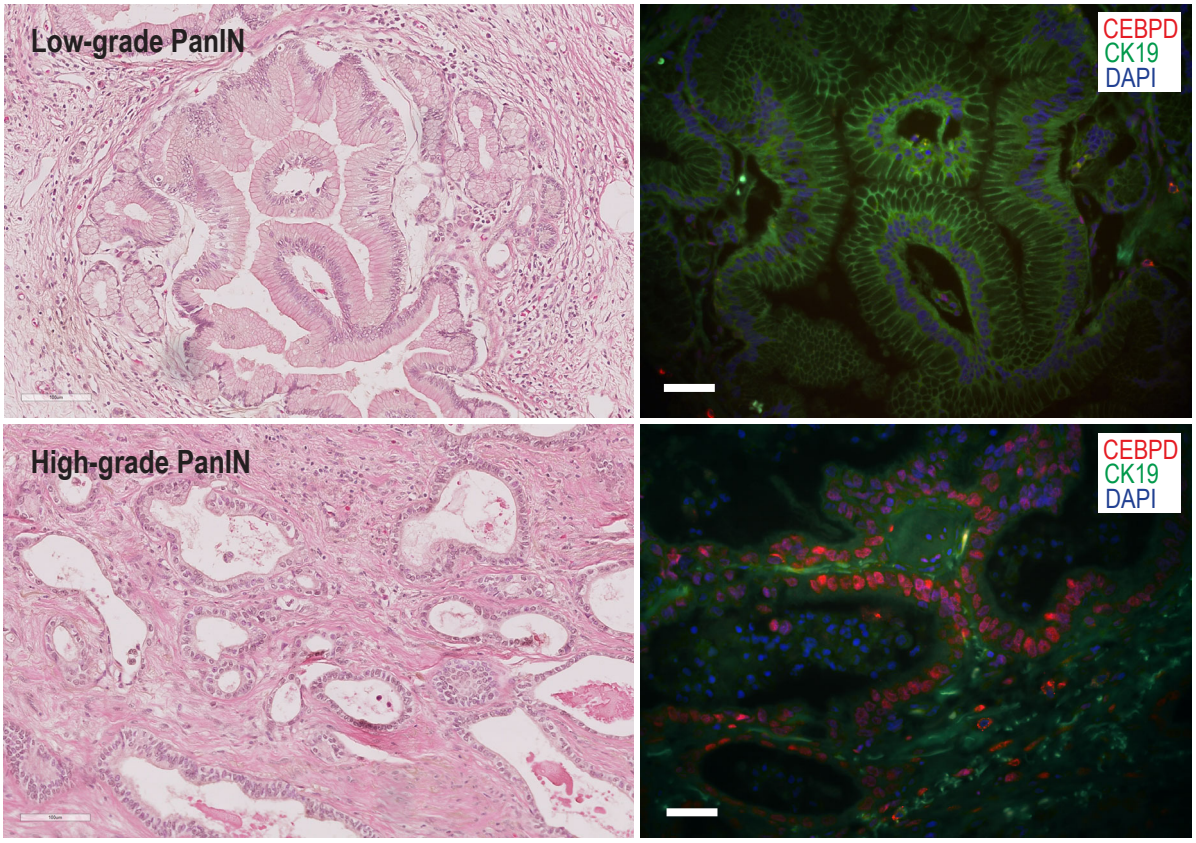
Low-grade PanIN
CEBPD
CK19
DAPI
High-grade PanIN
CEBPD
CK19
DAPI

B

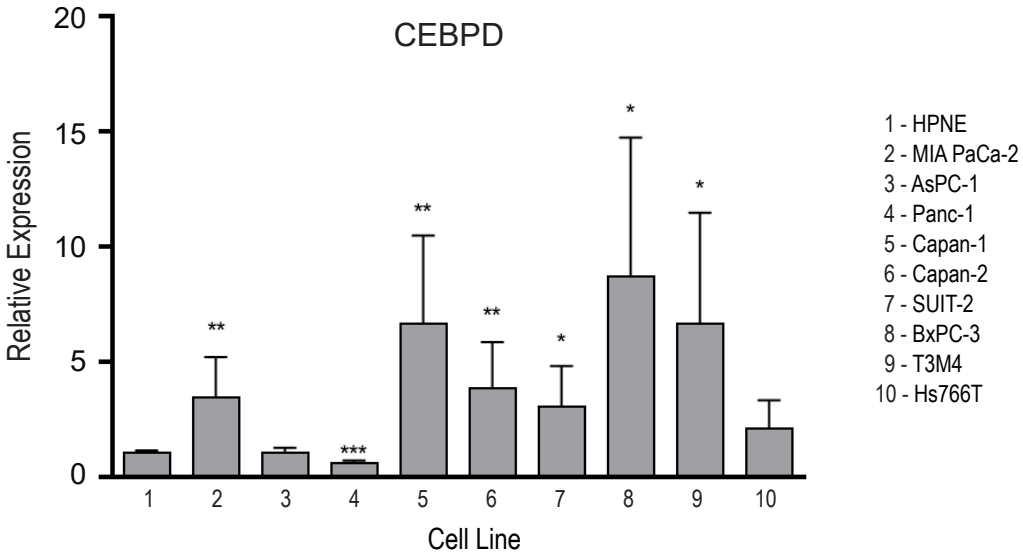
CEBPD
Relative Expression
Cell Line
0
5
10
15
20
1
2
3
4
5
6
7
8
9
10
1 - HPNE
2 - MIA PaCa-2
3 - AsPC-1
4 - Panc-1
5 - Capan-1
6 - Capan-2
7 - SUIT-2
8 - BxPC-3
9 - T3M4
10 - Hs766T

Supplemental Figure S12. C/EBPδ is upregulated in human high-grade pancreatic intraepithelial neoplasia and in 6 out of 9 human pancreatic cancer cell lines that are commonly used in research, Related to Figure 7

A. Left: H&E-stained histologic sections of low-grade and high-grade human pancreatic intraepithelial neoplasia; bars, 100 μm. Right: corresponding immunofluorescent images of C/EBPδ (CEBPD) and cytokeratin 19 (CK19); bars, 20 μm. **B**. Relative normalized expression of the C/EBPδ protein in human pancreatic cancer cell lines (n=9) in comparison to the average value of two untransformed normal pancreatic cell lysates (HPNE1a/1b shown in Fig. 7B). The densitometry results from C/EBPδ immunoblots were normalized to the corresponding loading controls (beta-actin, ACTB), and the bars represent the average expression from three technical immunoblot repeats (±SD). Statistical significance was calculated with unpaired t-tests and *P*-values <0.05 (∗), <0.01 (∗∗), <0.001 (∗∗∗), and <0.0001 (∗∗∗∗) were considered statistically significant.

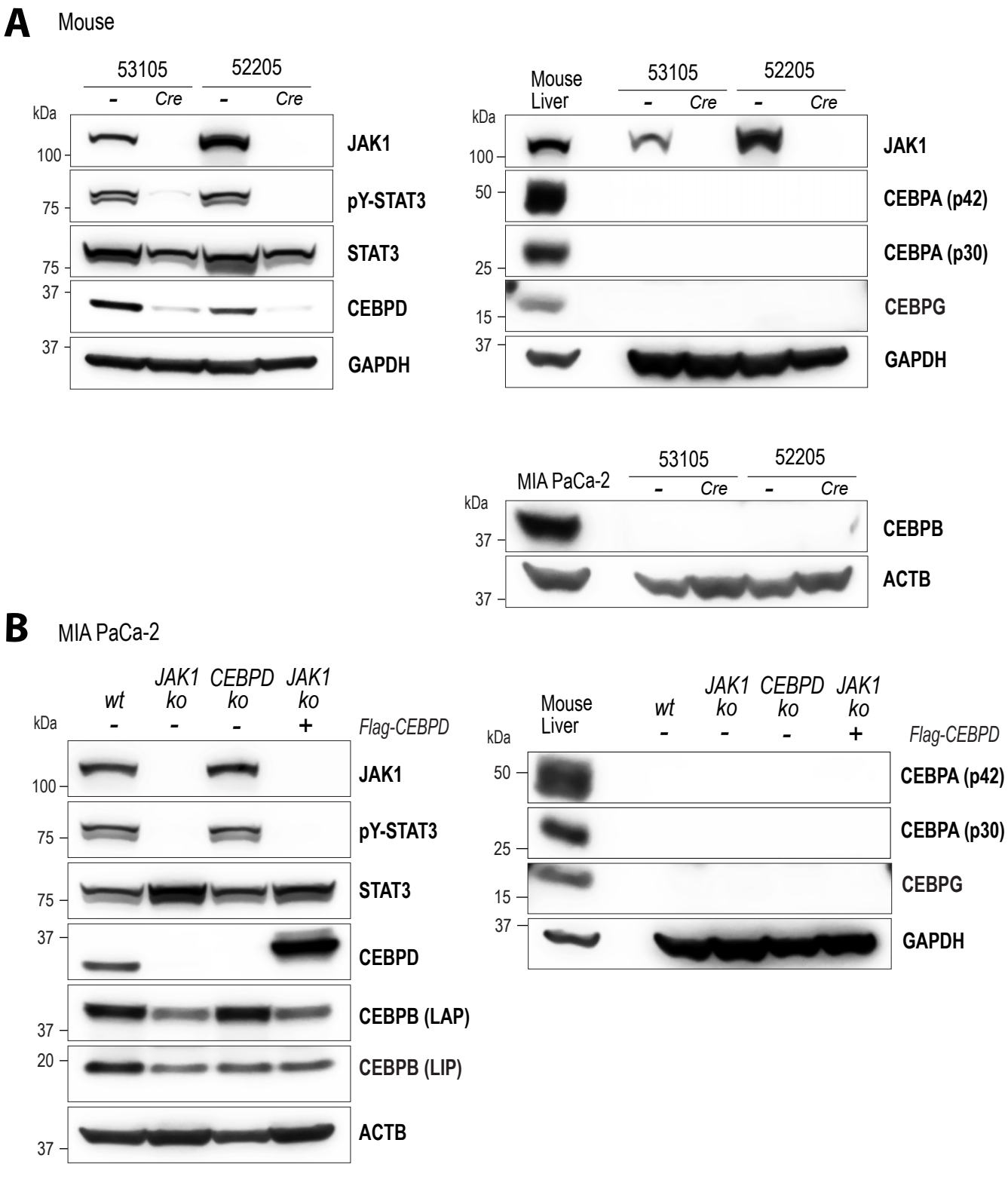
A
Mouse
53105
52205
-
Cre
-
Cre
kDa
100
75
75
37
37
JAK1
pY-STAT3
STAT3
CEBPD
GAPDH
Mouse Liver
53105
52205
-
Cre
-
Cre
kDa
100
50
25
15
37
JAK1
CEBPA (p42)
CEBPA (p30)
CEBPG
GAPDH
MIA PaCa-2
53105
52205
-
Cre
-
Cre
kDa
37
37
CEBPB
ACTB
B
MIA PaCa-2
wt
JAK1 ko
CEBPD ko
JAK1 ko
-
-
-
+
Flag-CEBPD
kDa
100
75
75
37
37
20
37
JAK1
pY-STAT3
STAT3
CEBPD
CEBPB (LAP)
CEBPB (LIP)
ACTB
Mouse Liver
wt
JAK1 ko
CEBPD ko
JAK1 ko
-
-
-
+
Flag-CEBPD
kDa
50
25
15
37
CEBPA (p42)
CEBPA (p30)
CEBPG
GAPDH

Supplemental Figure S13. JAK1-dependent expression of C/EBPδ and other CCAAT/enhancer binding proteins in mouse and human pancreatic cancer cells, Related to Figure 7

Immunoblot analyses assessing the expression of C/EBPα, C/EBPβ, C/EBPγ, and C/EBPδ in two isogenic mouse pancreatic tumor cell lines with or without JAK1 (**A**) and human MIA PaCa-2 cancer cells before and after the CRISPR/Cas9-mediated knockout of JAK1 and C/EBPδ (**B**). The analysis of CEBP family proteins in JAK1-deficient MIA PaCa-2 cancer cells with reinstated expression of C/EBPδ shows that expression of the LAP and LIP isoforms is controlled, in part, by JAK1 in a C/EBPδ-independent manner. Beta-Actin (ACTB) and GAPDH were used as loading controls.

A

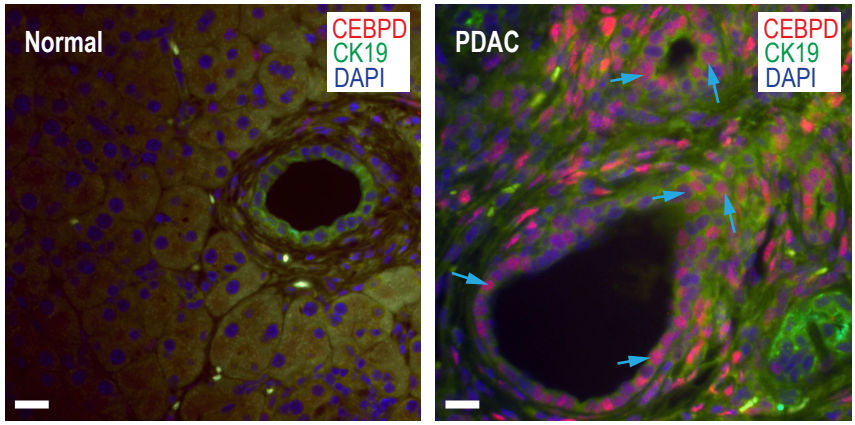
Normal
CEBPD
CK19
DAPI
PDAC
CEBPD
CK19
DAPI

B

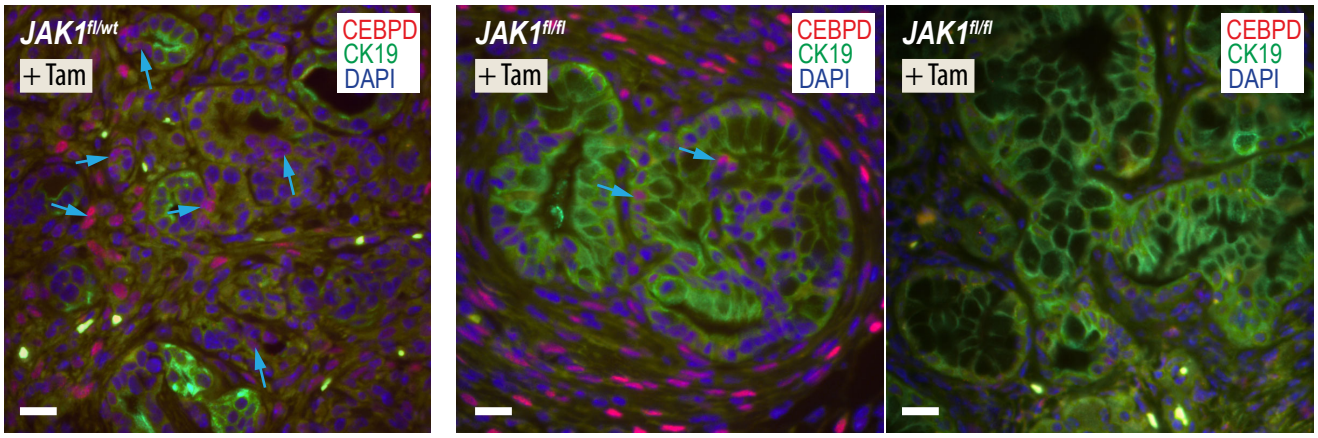
JAK1fl/wt
+ Tam
CEBPD
CK19
DAPI
JAK1fl/fl
+ Tam
CEBPD
CK19
DAPI
JAK1fl/fl
+ Tam
CEBPD
CK19
DAPI

Supplemental Figure S14. C/EBPδ is upregulated in mouse pancreatic tumors in a JAK1-dependent manner, Related to Figure 7

A. Left: H&E-stained histologic sections of low-grade and high-grade human pancreatic intraepithelial neoplasia; bars, 100 μm. Right: corresponding immunofluorescent images of C/EBPδ (CEBPD) and cytokeratin 19 (CK19); bars, 20 μm. **B**. Immunofluorescent staining of C/EBPδ (CEBPD) and cytokeratin 19 (CK19) in the normal mouse pancreas (left) and in a mutant KRAS-induced pancreatic tumor (Pdx1-Flp *FSF-Kras*^{G12D}, right); bars, 20 μm. Blue arrows point to the location of ductal tumor cells with pronounced nuclear expression of C/EBPδ. **C**. Nuclear expression of C/EBPδ in pancreatic tissues of Pdx1-Flp *FSF-Kras*^{G12D} *Rosa26*$^{CAG\text{-}FSF\text{-}CreERT}$ mice with a tamoxifen-induced (+Tam) heterozygous (*Jak1*$^{fl/wt}$, left) and homozygous deletion of JAK1 (*Jak1*$^{fl/fl}$, middle and right). The panels in the middle and right show images of a more advanced preneoplastic lesion (middle) and low-grade PanINs (right) in the Tam-treated JAK1 knockout; bars, 20 μm. These mice were treated with Tam around 160 days of age, i.e., after preneoplastic lesions started forming, and examined 40 days later.

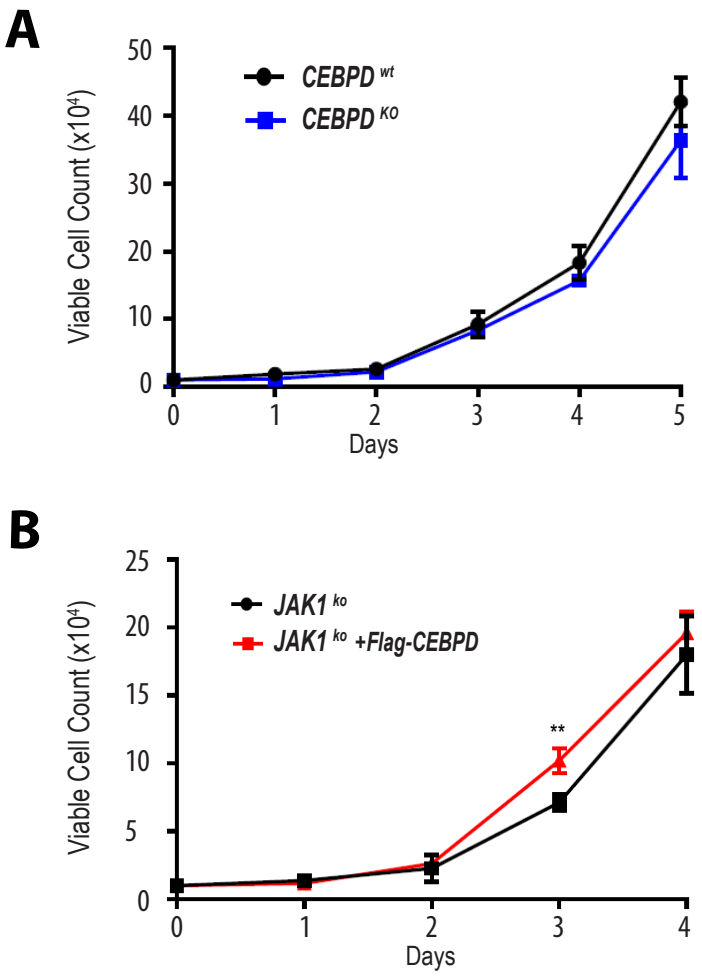
A
CEBPD wt
CEBPD KO
Viable Cell Count (x10⁴)
Days
B
JAK1 ko
JAK1 ko +Flag-CEBPD
**
Viable Cell Count (x10⁴)
Days

Supplemental Figure S15. Insignificant effects of a C/EBPδ knockout or its overexpression on the proliferation of MIA PaCa-2 cells in monolayer cultures, Related to Figure 7

A. Viable cell counts of parental MIA PaCa-2 cells (*CEBPD*^{wt}) and their unselected (i.e., pooled) CEBPD knockout derivatives (*CEBPD*^{KO}). **B**. Cell growth curves of JAK1-deficient (*JAK1*^{ko}) MIA PaCa-2 cells without and with exogenous expression of Flag-tagged C/EBPδ (+*Flag-CEBPD*). The data points shown in panels A and B represent mean values of cell counts ±SD. Statistical significance was calculated for each time point with t-tests; P-value <0.01 (**).

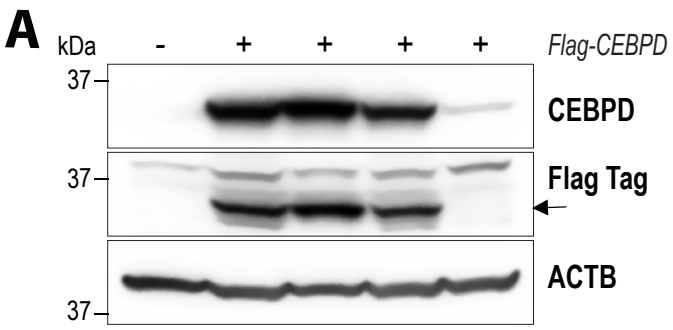
A
kDa
-
+
+
+
+
Flag-CEBPD
37
CEBPD
37
Flag Tag
37
ACTB

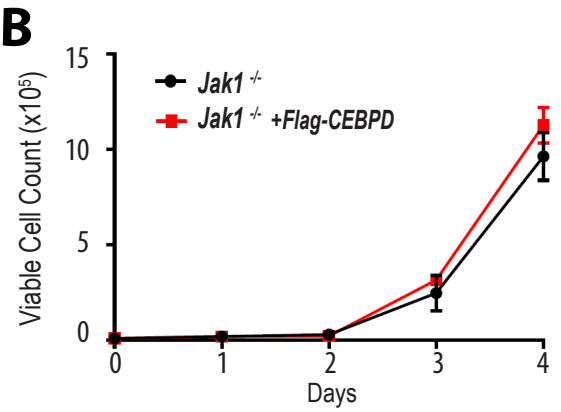
B
Viable Cell Count (x10⁵)
15
10
5
0
Jak1 -/-
Jak1 -/- +Flag-CEBPD
0
1
2
3
4
Days

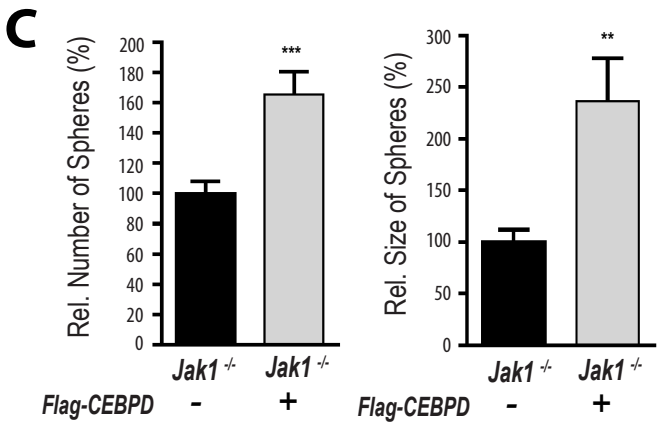
C
Rel. Number of Spheres (%)
200
180
160
140
120
100
80
60
40
20
0
***
Jak1 -/-
Jak1 -/-
Flag-CEBPD
-
+
Rel. Size of Spheres (%)
300
250
200
150
100
50
0
**
Jak1 -/-
Jak1 -/-
Flag-CEBPD
-
+

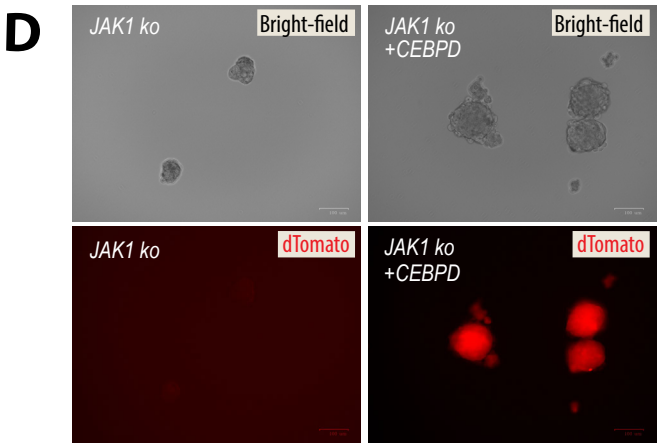
D
JAK1 ko
Bright-field
JAK1 ko
+CEBPD
Bright-field
JAK1 ko
dTomato
JAK1 ko
+CEBPD
dTomato

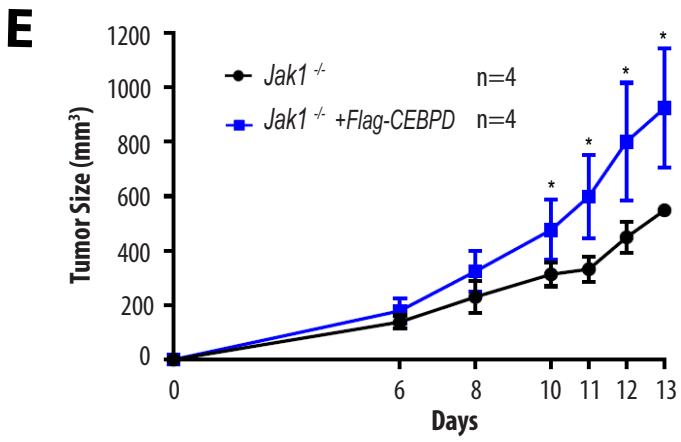
E
Tumor Size (mm³)
1200
1000
800
600
400
200
0
Jak1 -/-
n=4
Jak1 -/- +Flag-CEBPD
n=4
*
*
*
*
0
6
8
10
11
12
13
Days

Supplemental Figure S16. Upregulation of C/EBPδ in mouse pancreatic cancer cells with a conditional knockout of JAK1 accelerates the formation and growth of tumorspheres, Related to Figure 7

A. Immunoblot analysis to validate the expression of exogenous Flag-tagged C/EBPδ in mouse pancreatic cancer cells (n=4 independent pools of infected cells) with a conditional knockout of JAK1. Beta-actin (ACTB) was used as a loading control. **B**. Viable cell counts of JAK1-deficient tumor cells (*Jak1*$^{-/-}$) without and with exogenous expression of Flag-tagged C/EBPδ (+*Flag-CEBPD*). The data points shown represent mean values of cell counts ±SD. Statistical significance was tested for each time point with t-tests. **C**. Comparative analysis of the relative numbers and sizes of tumorspheres of JAK1-deficient pancreatic cancer cells following the expression of C/EBPδ (+*Flag-CEBPD*). **D**. Brightfield images of tumorspheres and corresponding fluorescent images of dTomato expression; bars, 100 µm**. E**. Growth curves of transplanted mouse pancreatic cancer cells with a Cre recombinase-mediated knockout of JAK1 (*Jak1*$^{-/-}$) with or without exogenous expression of Flag-tagged C/EBPδ; 4 biological repeats per tumor line. The data points shown represent mean values of measured tumor volumes ±SD. Statistical significance between tumor volumes was calculated with t-tests; P-values <0.05 (*).

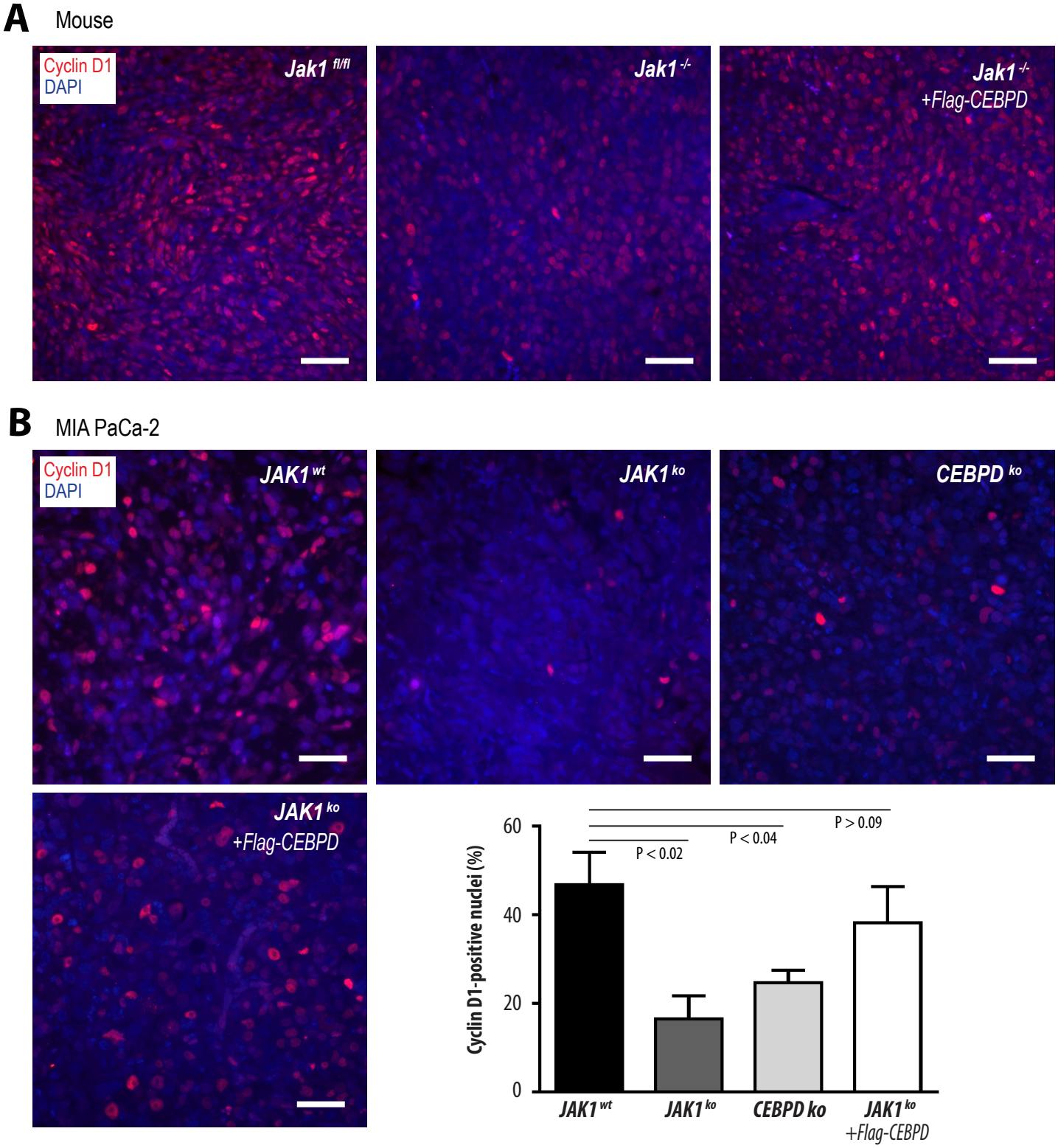
A
Mouse
Cyclin D1
DAPI
Jak1 fl/fl
Jak1 -/-
Jak1 -/-
+Flag-CEBPD
B
MIA PaCa-2
Cyclin D1
DAPI
JAK1 wt
JAK1 ko
CEBPD ko
JAK1 ko
+Flag-CEBPD
Cyclin D1-positive nuclei (%)
60
40
20
0
P < 0.02
P < 0.04
P > 0.09
JAK1 wt
JAK1 ko
CEBPD ko
JAK1 ko
+Flag-CEBPD

Supplemental Figure S17. The decelerated growth of JAK1-deficient mouse and human pancreatic cancer cells as well as C/EBPδ knockout MIA PaCa-2 cells in comparison to their parental JAK1 wildtype controls is accompanied by a reduced expression of Cyclin D1, Related to Figure 7

Immunofluorescence images of Cyclin D1 in mouse (**A**) and human (**B**) xenografted pancreatic cancer cells that lack JAK1 (*Jak1*$^{-/-}$, *JAK1*^{ko}) and their JAK1 wildtype parental controls (*Jak1*$^{fl/fl}$, *JAK1*^{wt}). Cyclin D1 is also reduced in MIA PaCa-2 cells that lack the JAK1 target C/EBPδ (*CEBPD*^{ko}). Reinstating the expression of C/EBPδ in mouse and human JAK1 knockout cells leads to a concomitant upregulation of Cyclin D1; bars, 50 μm. The box plot in panel B shows the statistically significant difference in the relative number of Cyclin D1-positive nuclei between the JAK1 and C/EBPδ knockouts and wildtype control MIA PaCa-2 cells and the rescue of Cyclin D1 expression in JAK1 knockout cells expressing exogenous C/EBPδ. Data are presented as the mean ±SD of three representative images (400x magnification) of non-overlapping tumor regions of each tumor line. Statistical significance was calculated with t-tests; *P*-values <0.05 (*) and <0.01 (**).

Supplementary Tables

Supplementary Table S1: PCR primers to genotype transgenes and genetically engineered alleles, Related to STAR Methods

Transgene / Allele	Primer #	Sequence (5' - 3')	bp
Pdx1-Cre	2268	CTG GAC TAC ATC TTG AGT TGC	580
	580	CAT CAC TCG TTG CAT CGA CC	
Chr9 (internal control)	2767	GAG ACA CTG TGA CCA AGG TAA C	~490
	2769	GCC AAG AGT TTG GCA CAT TAG C	
CAG-LSL-GFP	2004	GGC TCT AGA GCC TCT GCT AAC C	~270
	2211	GCC ATT GGG ATA TAT CAA CGG TG	
CAG-LSL-tTA	418	CTT CGC TAT TAC GCC AGC TGG	330
	2004	GGC TCT AGA GCC TCT GCT AAC C	
TetO-Kras^{G12D}	2366	GCC TGC GAC GGC GGC ATC TGC	320
	2367	GGG AAT AAG TGT GAT TTG CCT	
Jak1$^{fl/wt}$	2411	GAG ACA GGA TAC CTG GTG GCT TGG	350 (fl)
	2412	GTA GCA GTC CTG GAC ATT GAG TCC	250 (wt)
Jak1^{fl} (Δ PGK-neo)	2614	CCA TCA GCA CTA GCT GAG GTT C	285
	2615	CAC AAT GTA GCA AGA CCA AGC CAT G	
Jak1^{-} (Cre-recombined and Δ PGK-neo)	2717	GTA ACT AGC AGA AGG TCT GAT CTG	~230
	2615	CAC AAT GTA GCA AGA CCA AGC CAT G	
Pdx1-Flp	2524	AGA GAG AAA ATT GAA ACA AGT GCA GGT	620 (mu)
	2525	CGT TGT AAG GGA TGA TGG TGA ACT	
internal control	2526	AAC ACA CAC TGG AGG ACT GGC TAG G	300
	2527	CAA TGG TAG GCT CAC TCT GGG AGA TGA TA	
FSF-Kras^{G12D}	2528	CAC CAG CTT CGG CTT CCT ATT	270 (wt)
	2529	AGC TAA TGG CTC TCA AAG GAA TGT A	350 (mu)
	2530	GCG AAG AGT TTG TCC TCA ACC	
Kras^{G12D}	2600	GTC TTT CCC CAG CAC AGT GCA G	310 (wt)
(Flp recombined)	2602	GTT TTG TAG CAG CTA ATG GCT CTC	344 (mu)
Trp53^{R172H}	2598	AGC CTG CCT AGC TTC CTC AGG	290 (wt)
	2599	CTT GGA GAC ATA GCC ACA CTG	330 (mu)
LSL-p53^{R172H}	2598	AGC CTG CCT AGC TTC CTC AGG	290 (wt)
	2599	CTT GGA GAC ATA GCC ACA CTG	270 (mu)
	2581	AGC TAG CCA CCA TGG CTT GAG TAA GTC TGC A	
Rosa26$^{CAG-FSF-CreERT2}$	2729	CCC AAA GTC GCT CTG AGT TGT TAT C	550 (wt)
	2730	GAA GGA GCG GGA GAA ATG GAT ATG	~420 (mu)
	2731	CCA GGC GGG CCA TTT ACC GTA AG	
Jak2$^{fl/wt}$	1743	ATT CTG AGA TTC AGG TCT GAG C	230 (wt)
	1744	CTC ACA ACC ATC TGT ATC TCA C	310 (fl)

Supplementary Table S2: Primary and secondary antibodies for immunostaining, Related to STAR Methods

Primary Antibodies	SOURCE	IDENTIFIER	DILUTION
α-GFP	Avēs Labs	GFP-1020	1:1000
α-CK19	Developmental Studies Hybridoma Bank	TROMAIII	1:100
α-panCK	Dako/Agilent	M3515	1:400
α-pSTAT3	Cell Signaling	#9145	1:100 (mouse) 1:200 (human)
α-pSTAT5	Cell Signaling	#9351	1:1000
α-Ku80	Cell Signaling	#2180	1:100
α-CEBPD	Abcam	#ab245214	1:1000
α-Cyclin D1	Abcam	#ab16663	1:100
α-Ki67	Abcam	#ab15580	1:500
Secondary Antibodies	**SOURCE**	**IDENTIFIER**	**Dilution**
Alexa Fluor 488 goat anti-chicken	Invitrogen	A11039	1:1000
Alexa Fluor 488 donkey anti-rat	Invitrogen	A21208	1:1000
Alexa Fluor 594 donkey anti-rabbit	Invitrogen	A21207	1:1000
Alexa Fluor 555 goat anti-rabbit	Invitrogen	A21429	1:1000
Alexa Fluor 555 goat anti-mouse	Invitrogen	A21422	1:1000
Envision+/HRP-anti-rabbit	Dako	K400311-2	1:200

Supplementary Table S3: gRNA and shRNA sequence information, Related to STAR Methods

shRNA	Target Sequence	Species	Source	Publication
shJAK2	GCTTTGTCTTTCGTGTCATTA	Human	TRCN0000003180	Neilson et al., 2007
shJAK1	GAGACTTCCATGTTACTGATT	Human	TRCN0000003102	Neilson et al., 2007
shJAK1	CTTGGCTACCTTGGAAACTTT	Human	TRCN0000003105	Neilson et al., 2007
gRNA	**Target Sequence**	**Species**	**Source**	**Publication**
JAK1	CATCTATTCTGGGACCCTGA	Human	Synthego	Designed for this project
CEBPD	GCCGTCCAGGCTGAAGAGCG	Human	Synthego	Designed for this project
CEBPD	CCCGGTTCGTAGAAGGGCGC	Human	Synthego	Designed for this project
CEBPD	CTCTCGTCGTCGTACATGGC	Human	Synthego	Designed for this project

Supplementary Table S4: Primary and secondary antibodies for immunoblotting, Related to STAR Methods

Primary Antibodies	SOURCE	IDENTIFIER	DILUTION
α-JAK1	Cell Signaling	#50996	1:1000
α-JAK2	Cell Signaling	#3230	1:1000
α-pY-STAT1	Origene	#TA309955	1:1000
α-STAT1	Santa Cruz	#sc-592	1:200
α-STAT1	Cell Signaling	#14994	1:1000
α-pY-STAT3	Cell Signaling	#9145S	1:1000
α-STAT3	Cell Signaling	#9139S	1:1000 1:200 IP
α-pY-STAT5	Cell Signaling	#9351S	1:1000
α-STAT5	Santa Cruz	#sc-836	1:200
α-pY-STAT6	Abcam	#ab54461	1:1000
α-pY-STAT6	Cell Signaling	#9361	1:1000
α -STAT6	Santa Cruz	#sc-981	1:200
α-GAPDH	Cell Signaling	#5174S	1:10000
α-GFP	Avēs Labs	#GFP-1020	1:5000
α-ACTB	Santa Cruz	#sc-47778	1:200
α-CEBPD	Abcam	#ab245214	1:1000
α-CEBPD	Santa Cruz	#sc-135733	1:100
α-CEBPA	Santa Cruz	#sc-166258	1:100
α-CEBPB	Abcam	#ab32358	1:1000
α-CEBPG	Invitrogen	#PA5-121085	1:1000
α-FLAG	Thermo Fisher	#PA1-984B	1:1000
α-pERK1/2	Cell Signaling	#9101S	1:1000
α-ERK1/2	BD Transduction Laboratories	#610123	1:1000
α-pT308-AKT	Cell Signaling	#4056	1:1000
α-pS473-AKT	Cell Signaling	#9271	1:1000
α-AKT	Cell Signaling	#9272	1:1000
α-EpCAM	Cell Signaling	#93790S	1:1000
α-E-cadherin	Cell Signaling	#3195	1:1000
α-N-cadherin	Cell Signaling	#14215	1:1000
α-VIMENTIN	Cell Signaling	#5741	1:1000
α-SNAIL	Cell Signaling	#3879T	1:1000
α-SLUG	Cell Signaling	#9585T	1:1000
α-ZEB1	Cell Signaling	#70512T	1:1000
α-TWIST	Santa Cruz	#sc-81417	1:100
α-TWIST	Cell Signaling	#46702S	1:500
α-p110a	Cell Signaling	#4249	1:1000
α-p85 (p50/p55)	Upstate	#06-195	1:1000
Secondary Antibodies	**SOURCE**	**IDENTIFIER**	**DILUTION**
Digital anti-Mouse-HRP	KwikQuant	R1005	1:1000
Digital anti-Rabbit-HRP	KwikQuant	R1006	1:1000
Goat anti-Chicken IgY-HRP	Santa Cruz	#sc-2428	1:1000
Goat anti-Rat IgG-HRP	Santa Cruz	#sc-2006	1:1000

Supplementary Table S5: nCounter elements design details, Related to STAR Methods

Gene Name	Accession	Target Sequence
Car11	NM_009800.4	TTTGTCAATGTGGCTGGCAGTTCCAACCCATTCCTCAGTCGCCTCCTCAAC CGGGACACTATCACCCGAATCTCCTACAAAAATGATGCCTACTTTCTTC
Cebpd	NM_007679.4	AAGGAACACGGGAAAGCATGACTAATTCATGTGTGTGATCCCAGAGTAGGC TGACCTGGGGCGGAGAACAGTTGGCCTAACTTTTAGGTGGTTGCCGAAG
Clca3a1	NM_009899.3	CTTCTGGTGGAACTTCAATTTGCCATGGACTCCAGGCAGGATTTCAGGCAA TTACCTCCAGTGACCAGAGCACTTCCGGTTCTGAGATCGTATTGCTGAC
Ifitm3	NM_025378.2	AACCGAAACTGCCGCAGAAAGGGCAGACCCGCAGCGCGCTCCATCCTTTG CCCTTCAGTGCTGCCTTTGCTCCGCACCATGAACCACACTTCTCAAGCCT
Isg15	NM_015783.3	TATGAGGTCTTTCTGACGCAGACTGTAGACACGCTTAAGAAGAAGGTGTCC CAGCGGGAACAAGTCCACGAAGACCAGTTCTGGCTGAGCTTCGAGGGAA
Oasl2	NM_011854.2	TCTCCAGAAACCTCTTAGAATGGAAAACTAACCCAAGCCAGACATTTCACCG AGACTCAGCGGTCCTGGACTTAACAAGCCTTTCACATCATTCTGCATG
Txnip	NM_023719.1	CCTGAGTGCTGCGATCAAAGGCCCAGCTTGGTTATTGCTTTTGAGGCTTTC TCCCAACGCACAGACTTGTGTAATTCTAACACTAATCCTGTGAAGGGTT
Gpm6b	NM_023122.2	GTGGCAATTCTTGAGCAACACTTCTCCACCAACACCAGTGACCATGCCTTG CTGAGTGAAGTGATCCAACTGATGCAGTATGTTATCTATGGAATCGCCT
Osmr	NM_011019.3	GAAGAAGCTGTGCGTTGGAACTGGACGTCTGATATCCCTTTGGAGTGTGTC AAACATTTCATAAGAATCAGGGCTCTGGTAGATGACACCAAGTCCCTTC
Stat3	NM_011486.4	ATCAAATCTGTAAAAGAGATCCGAGAGCTGTGGCTTGGCCTCTGGTTCAAA CACAAAGGCTAGAGAGAACCTAGATATCCCTGGGTTTTGTTTACCCAGT
Socs3	NM_007707.3	GAGGCTGGTGAGCTGGCCGCCTTTTCCAACACCGAAGGGAGGCAGATCAA CAGATGAGCCATCTTGGAGCCCAGGTTTCCCTGGAGCAGATGGAGGGTTC
Pdgfra	NM_011058.2	ATTGCAATGCAAAAGTTGAGAAGAGGACTTGGGTGATGTGGAGAGAGAAAG TTCCCGAGGCCGAGGGCCTTGGTAAGCCTGTGTGGATGACTGGGATACT
Tgfbi	NM_009369.4	TCTGTGTTCAAAGATGGTGTCCCTCGCATCGACGCCCAGATGAAGACTTTG CTTCTGAACCACATGGTCAAAGAACAGTTGGCCTCCAAGTATCTGTACT
Fos	NM_010234.2	TCCAGTCCTCACCTCTTCCAGAGATGTAGCAAAAACAAAACAAAACAAAACA AAAAACCGCATGGAGTGTGTTGTTCCTAGTGACACCTGAGAGCTGGTA
Map3k8	NM_007746.2	GGTTCTCATTTCTCAGGTGGTGGGACTAGACAGAGGGAGTGGCAAGCTCA GGGAAGGATCATTTCTGGTGATAATTCCATTCACTTTGCACTTTGATGGG
Bmf	NM_138313.3	GACTTTGGAAGTAACAGACAATGTTTAGACCATGGAAACTGCAGAGCTGAC ACATCTTGAATCTCCCTTTAGCTTTCAGCTAGGCCAGAAAGGAGAGTTC
Edc3	NM_153799.3	CTTTATAGTTGCCCTCCTCAGGTGTATAGTTGGAACTAGTGGCCTGTCTCAA ACATGCCAAAAATGAGCCCAGTTCTAGATGACAGTAGTGGGATTCAGC
Ralb	NM_022327.5	CACCAGCTCTAGGGTCGTAATGTTGGAGATCAGGAATATTGGTTGTGATGA CAAGAAAGAGCCCACTTACTCCTCCTCGTTCTAGGACACGGTCATCTTT
Cox6b1	NM_025628.2	TGGTACCGGCGTGTGTACAAGTCCCTCTGTCCCGTGTCATGGGTCTCAGCC TGGGATGACCGCATAGCTGAAGGCACATTTCCTGGGAAGATCTGACCTG
Tbp	NM_013684.3	GTGGCGGGTATCTGCTGGCGGTTTGGCTAGGTTTCTGCGGTCGCGTCATTT TCTCCGCAGTGCCCAGCATCACTATTTCATGGTGTGTGAAGATAACCCA
Bcl3	NM_033601.3	CCCCACTTAATCTCAGGCACCCAGGTTCCCTGTCTGGAATCCACCAGATAC TCAATTCTTTGAGTGGAGGAACCAAAGGACAGCCAGCCTCTCCTCTGCC
Zfp467	NM_001085415.1	CGAAGTTCTGACCCTCATCCTGCCTTTCCTGACAGATTTGGGAGACTCATAT CTGGAGACTTAGTGGGTTTTCAACATTCACACCTAAGTTGCTGCCAAA
Mmp10	NM_019471.2	CAGACTTAGATGCTGCCTATGAGGCTCACAACACGGACAGTGTTCTGATTTT TAAAGGAAGTCAGTTCTGGGCAGTCCGAGGAAATGAAGTCCAAGCAGG
Mmp13	NM_008607.1	ACAGTGACCTCCACAGTTGACAGGCTCCGAGAAATGCAATCTTTCTTTGGC TTAGAGGTGACTGGCAAACTTGATGATCCCACCTTAGACATCATGAGAA
Mmp19	NM_021412.2	CGACGGACTCATTTCTTCAAGGGAAACAAGGTGTGGCGGTATGTGGATTTC AAGATGTCTCCTGGCTTTCCCATGAAATTCAACAGAGTAGAGCCCAACC
Mmp2	NM_008610.2	AGTTAACCAGCCTTCTCCTTCACCTGGTGACTTCAGATTTAAGAGGGTGGCT TCTTTTTGTGCCCAAAGAAAGGTGCTGACTGTACCCTCCCGGGTGCTG
Mmp3	NM_010809.1	TCTTTGTGAAAGGAAGTGCTTTGTTCAGCATGTGCTATGGCAGAACCAAACA GGAGCTATGGATGACACCAGTCAACGTCAAGTTGTCAAAGGATGTTCA
Jak1	NM_146145.2	CATAGCAAAGGACTGTGCCGCTGGCATATTGATCTCAGATAAAAACTTGTG GACTTGGCTGACACTCTCCCTTGCCCTGAAATCTCAATGTCTATTCAGT
Jak2	NM_008413.3	GTGCTGGAACAACAATGTGAGCCAGCGTCCCTCCTTCAGGGACCTTTCCCT TCGGGTGGATCAAATCCGGGACAGTATAGCTGCGTGAAAGAGATGGCCT